Available online at www.sciencedirect.com
ScienceDirect
Journal of Photochemistry and Photobiology A: Chemistry 194 (2008) 308–317
Journal of Photochemistry and Photobiology A:Chemistry
www.elsevier.com/locate/jphotochem

Optical spectroscopic characteristics and TD-DFT calculations of new pyrrolo[1,2-b]pyridazine derivatives

Marilena Vasilescu [a,*], Rodica Bandula [a], Oana Cramariuc [b], Terttu Hukka [b], Helge Lemmetyinen [b], Tapio T. Rantala [c], Florea Dumitrascu [d]

[a] *Institute of Physical Chemistry, Romanian Academy, Splaiul Independentei 202, 060021 Bucharest, Romania*
[b] *Institute of Materials Chemistry, Tampere University of Technology, 33101 Tampere, Finland*
[c] *Institute of Physics, Tampere University of Technology, 33101 Tampere, Finland*
[d] *Centre of Organic Chemistry, Romanian Academy, Splaiul Independentei 202, 060021 Bucharest, Romania*

Received 14 March 2007; received in revised form 27 August 2007; accepted 28 August 2007
Available online 1 September 2007

Abstract

Five new pyrrolo[1,2-b]pyridazine derivatives: 5,6-dicarbomethoxy-2,7-dimethylpyrrolo[1,2-b]pyridazine (**I**), 5,6-dicarbomethoxy-7-methyl-2-phenylpyrrolo[1,2-b]pyridazine (**II**), 5,6-dicarbomethoxy-7-ethyl-2-phenylpyrrolo[1,2-b]pyridazine (**III**), 5-carboethoxy-7-methyl-2-phenylpyrrolo[1,2-b]pyridazine (**IV**) and 7-ethyl-2-phenylpyrrolo[1,2-b]pyridazine (**V**), with aryl or methyl substituents in pyridazinic ring and with alkyl, aryl and/or carbometoxy in the pyrrolic ring have been investigated by spectroscopic methods and electronic structure calculations. UV–vis absorption together with steady-state and time-resolved fluorescence measurements have been conducted in cyclohexane, *n*-hexane (as inert solvents), and in solid state to evidence comparatively the effect of the structure of the compounds on the absorption and fluorescence properties. All five compounds have an intense fluorescence with high quantum yields. The intense fluorescence is evidenced also in solid state. The electronic structure calculations have been performed in the framework of density functional theory (DFT) and time dependent DFT (TD-DFT) in order to elucidate the differences observed in absorption spectra as an effect of the substituents.

Keywords: Pyrrolo[1,2-b]pyridazine; Fluorescence; Solid state; DFT; TD-DFT

1. Introduction

Heterocycles have at least one lone pair of nonbonding *n* electrons, which can be excited into a π* orbital by an electronic promotion which is commonly referred to as *n*–π* transition. If the lowest energy absorption band of a compound corresponds to a *n*–π* transition the compound is generally not fluorescent. However, if the lowest energy absorption band corresponds to a π–π* transition the compound is fluorescent. Because of their possible high fluorescence quantum yields aromatic heterocycles are actively studied in connection with several application areas such as emissive materials, organic luminophores and organic thin film nanostructures. In this context, the efficient electroluminescence reported for organic thin film devices [1–4] promises to transform the flat panel display industry by replacing liquid crystal displays with an entirely new generation of efficient, emissive, full colour flat panels based on light-emitting organic devices. More recent developments also point out that organic thin films can be used as thin film transistors (TFTs) [5,6], eventually replacing amorphous or polysilicon TFTs currently used in the back planes of active matrix liquid crystals. Additionally, also many, somewhat less conventional applications, are reported for organic thin films deposited in vacuum [7–9].

The absorption and fluorescence spectra of heterocycles are extremely solvent sensitive and depend, on one hand, on the nature of the substituents at the heterocycle, and on the other hand, on the positions of the substituents. In the case of five atom heterocycles the position of the substituents can be even considered critical for their fluorescence properties, proven by the fact that indole (2,3-benzopyrrole) is fluorescent, whereas pyrrole is not fluorescent. Fused heterocyclic rings offer very interesting optical properties. Indolizine is the simplest heteroaromatic

* Corresponding author.
E-mail address: mvasilescu@chimfiz.icf.ro (M. Vasilescu).

1010-6030/$ – see front matter © 2007 Elsevier B.V. All rights reserved.
doi:10.1016/j.jphotochem.2007.08.029

planar molecule containing both a π-excessive pyrrole and a π-deficient pyridine ring with one bridgehead nitrogen, the whole system being isomeric with indole. Indolizines are fluorescent both in solution and in solid state [10,11]. Oxazolones, which result from the condensation of pyridazine with oxazole are intense fluorescent both in solution and solid state and their fluorescence depends on both substituents and solvent [12,13]. Pyrrolo[1,2-b]-pyridazines, which result from the condensation of pyridazine with pyrrole also have special photo-physical properties [14–17] evidenced by their intense fluorescence in solution and solid state. Due to the applicability of their derivatives in pharmaceutical industry, having antiviral [18], anticancer [19] and other biological activities [20–25], the study of these compounds and the investigation of their special fluorescence properties is an important research subject.

The colour and intensity of the emission of the heterocycle compounds can be tuned by modifying their structural characteristics. In this context, the investigation of the relationship between the optical properties of pyrrolopyridazines and the nature and positions of substituents, or the expansion of their π–π conjugated system is both interesting and important. In this study we present the spectroscopic characterization (absorption and fluorescence) of five new pyrrolo[1,2-b]pyridazine derivatives designed with the aim of obtaining new fluorescent probes with high absorption coefficients, emission in the visible range and high fluorescence quantum yields. The derivatives under study have aryl or methyl substituents at the pyridazinic ring and alkyl, aryl and/or carbometoxy at the pyrrolic ring. The UV–vis absorption and both steady-state and time-resolved fluorescence measurements were conducted in cyclohexane, *n*-hexane (as inert solvents) and in solid state to evidence comparatively the effect of the structure of the compounds on the absorption and fluorescence properties. Density functional theory (DFT) and time dependent DFT (TD-DFT) calculations have been performed in order to elucidate the differences observed in absorption spectra as an effect of the substituents.

2. Experimental

2.1. Materials and solutions

The molecular structures of the pyrrolo[1,2-b]pyridazine derivatives **I–V** were confirmed by elemental analysis, IR spectroscopy, mass and NMR spectrometry. Their synthesis and chemical properties have been communicated [26] and will be published elsewhere. Solvents (spectroscopic grade) from Merck were used.

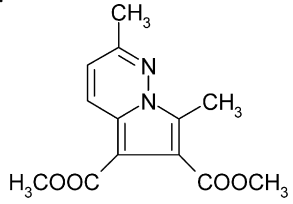

I $C_{13}H_{14}N_2O_4$

5,6-Dicarbomethoxy-2,7-dimethylpyrrolo[1,2-b]pyridazine, **I**

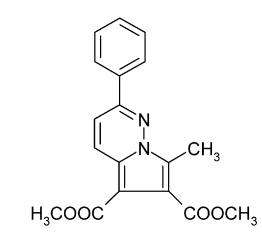

II $C_{18}H_{16}N_2O_4$

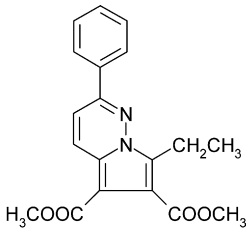

III $C_{19}H_{18}N_2O_4$

5,6-Dicarbomethoxy-7-methyl-2-phenylpyrrolo[1,2-b]pyridazine, **II**

5,6-Dicarbomethoxy-7-ethyl-2-phenylpyrrolo[1,2-b]pyridazine, **III**

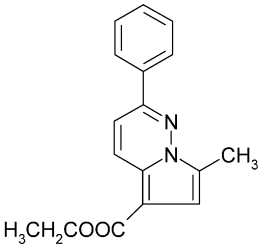

IV $C_{17}H_{16}N_2O_2$

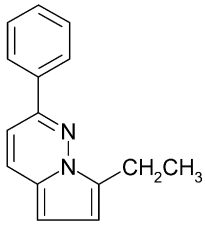

V $C_{15}H_{14}N_2$

5-Carboethoxy-7-methyl-2-phenylpyrrolo[1,2-b]pyridazine, **IV**

7-Ethyl-2-phenylpyrrolo[1,2-b]pyridazine, **V**

2.2. Methods

The fluorescence spectra (emission and excitation) were recorded at 23 °C with a Fluorolog Jobin Yvon Spex spectrofluorimeter and corrected automatically for instrumental effects (artifacts).

The relative fluorescence quantum yields were determined by comparison to a diluted quinine bisulfate solution in 0.1N H_2SO_4 having a 0.55 absolute quantum yield [27]. The fluorescence lifetimes of the phenylpyrrolo[1,2-b]pyridazine derivatives were measured at 21 °C using a single photon counting technique. The excitation setup uses a mode-locked Nd-YAG laser (Spectra Physics Model 379.344S) and a dye-laser. The excitation wavelength was 300 nm. The experimental method is described in [28]. The data was fitted by a single- or a double-exponential function ($F(t) = a_1\exp(-t/\tau_1) + a_2\exp(-t/\tau_2)$). The quality of the data fit was judged using statistical parameters and graphical tests. The data have been fitted using nonlinear least squares method. The reduced chi-squared values were close to 1. The weighted residuals were low and uniform distributed around zero.

The absorption spectra were recorded at 23 °C with a Shimadzu UV–vis 2501 PC spectrophotometer.

For the spectroscopic measurements of the compounds in solid state a concentrated solution in cyclohexane was evaporated on a quartz plate, thus obtaining a very thin layer of crystalline compound. The measurements were performed by

transmission in the case of UV–vis absorption and by frontal face illumination in the case of fluorescence. In addition, also powder solid compounds were measured for comparing the fluorescence intensity values.

3. Results

3.1. Experimental and calculated UV–vis absorption spectra

The studied compounds, although relatively similar in molecular structure, exhibit clear differences in their experimental UV–vis absorption spectra as can be seen from Fig. 1. The absorption maxima of the five derivatives in cyclohexane and the corresponding molar extinction coefficients, ε, are summarized in Table 1. The influence of the substituents on the spectra presented in Fig. 1 is analyzed in detail below.

3.2. Substitution by methyl or phenyl at the pyridazinic ring

Due to the planarity of compound **II**, as proven by X-ray analysis and DFT calculations, the replacement of the methyl group (compound **I**) by phenyl (compound **II**) extends the conjugation of the π-electrons from the pyridazinic and pyrrolic rings to the benzene ring as well. A bathochromic shift of $\Delta_{max} = 17$ nm for the low-energy band ($S_0 \rightarrow S_1$* transition) of **II** and the modification of the ε values (higher ε values for **II**) are observed when comparing **I** and **II**.

3.3. Substitution by methyl or ethyl at the pyrrolic ring

The replacement of the methyl group (compound **II**) with the ethyl group (compound **III**) at the pyrrolic ring induces very small spectral modifications. In the case of derivative **III**, the low-energy band is a slightly blue-shifted and the influence on the ε values is small (see also Table 1).

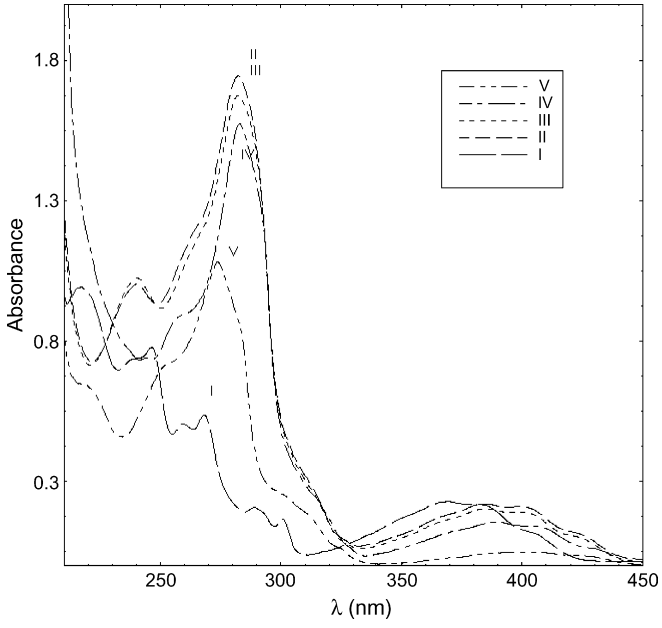

Fig. 1. Experimental absorption spectra of compound **I–V** in cyclohexane.

Table 1
Absorption (λ_{abs} and ε) for the pyrrolo[1,2-b]pyridazine derivatives in cyclohexane and solid state along

	λ_{abs} (nm)	ε (L mol^{-1} cm^{-1}) × 10^3	λ_{abs} (nm) solid
I	380.4	4.35	443
	370.0	4.53	380
	300.6	3.29	355
	289.2	4.11	298
	268.2	10.73	
	246.4	15.54	242
	217.2	19.86	
	397.6	4.17	430
II	384.8	4.37	409
	282.4	34.92	293
	240.4	20.07	239
	399.4	3.79	439
III	386.0	4.01	393
	282.0	33.55	287.5
	240.4	20.51	243
	390.0	3.08	433
IV	283.0	31.51	400
	244.6	14.78	289
			253
	405.4	0.95	439
V	274.0	21.63	299
			242

3.4. Substitution by esters at the pyrrolic ring

Comparing **III** with **V** and **II** with **IV** one can conclude that ester substituents play an important role in the distribution of energy in the absorption spectra, evidenced by hypsochromic shifts and increased ε values.

DFT and TD-DFT calculations were performed for obtaining detailed informations about the structures of the studied pyrrolopyridazine derivatives and for assessing the nature of the differences observed in their experimental absorption spectra. Both the B3LYP exchange-correlation (xc) hybrid functional [29–33], as employed by Mitsumori et al. for pyrolopyridazine derivatives [15] and the PBE0 [34,35] xc hybrid functional employed by Cossi and Barone [36] were used in the calculations. In addition, also several basis sets, i.e. SVP [37,38], DZP [37] and TZVP [39], were employed for assessing the influence of the basis set size. Also several calculations with the COSMO continuum solvatation model were performed in order to assess the influence of non-polar solvents on the absorption spectra of the compounds. The Turbomole computational software [40] was used in all calculations.

Independent on the computational setup, the calculations yield minimum energy structures of **II–IV** in which the almost perfect co-planarity of the phenyl and pyridazinic rings is an important structural characteristic to be considered in the interpretation of the electronic and spectroscopic properties. This feature can significantly influence the electronic structure of

the compounds by allowing the extension of the π-conjugation, thus lowering the energies of the MOs involved in the conjugation. Comparison of the molecular orbitals (MOs) energies in Table 2 and analysis of Fig. 2 reveals that extended π-conjugation can successfully explain the changes in the energies of the LUMO + 1, LUMO and HOMO orbitals but not the ones of HOMO-1. The energy of the LUMO + 1 orbital is lowered more than twice when comparing **I** and **II** due to the delocalization and high amplitude of the orbital on the phenyl ring of **II**. At the same time LUMO is less delocalized on the phenyl, having lower amplitude, and thus a smaller decrease in energy. The HOMO orbital, which has almost zero amplitude on the phenyl ring in compound **II**, shows little to no change in energy.

Also the other substituents at the pyridazinic ring are inducing sometimes significant changes in the electronic structure of **I–V**, as evidenced by the MO energies given in Table 2. Additionally, the analysis of Table 2 reveals that while the LUMO orbitals are less influenced by the change of the xc functional, the HOMOs are underbound by B3LYP (<0.5 eV) as compared

Table 2
Energies in eV of the MOs of **I–V**, calculated with the B3LYP and PBE0 hybrid xc functionals and several basis sets

MO	Method	I	II	III	IV	V
LUMO + 1	B3LYP/SVP	−0.59	−1.23	−1.26	−1.15	−0.69
	PBE0/SVP	−0.64	−1.23	−1.22	−1.15	−0.68
	PBE0/DZP	−0.57	−1.18	−1.21	−1.10	−0.65
	PBE0/TZVP	−0.74	−1.33	−1.35	−1.24	−0.78
LUMO	B3LYP/SVP	−1.78	−1.99	−2.00	−1.75	−1.53
	PBE0/SVP	−1.86	−2.00	−1.98	−1.76	−1.53
	PBE0/DZP	−1.80	−1.94	−1.96	−1.71	−1.49
	PBE0/TZVP	−1.96	−2.08	−2.09	−1.83	−1.59
HOMO	B3LYP/SVP	−5.82	−5.87	−5.86	−5.70	−5.37
	PBE0/SVP	−6.16	−6.22	−6.21	−6.05	−5.71
	PBE0/DZP	−6.09	−6.16	−6.16	−5.98	−5.66
	PBE0/TZVP	−6.21	−6.26	−6.25	−6.07	−5.72
HOMO-1	B3LYP/SVP	−6.76	−6.51	−6.49	−6.40	−6.11
	PBE0/SVP	−7.16	−6.89	−6.86	−6.77	−6.47
	PBE0/DZP	−7.08	−6.83	−6.81	−6.71	−6.43
	PBE0/TZVP	−7.21	−6.92	−6.90	−6.79	−6.48

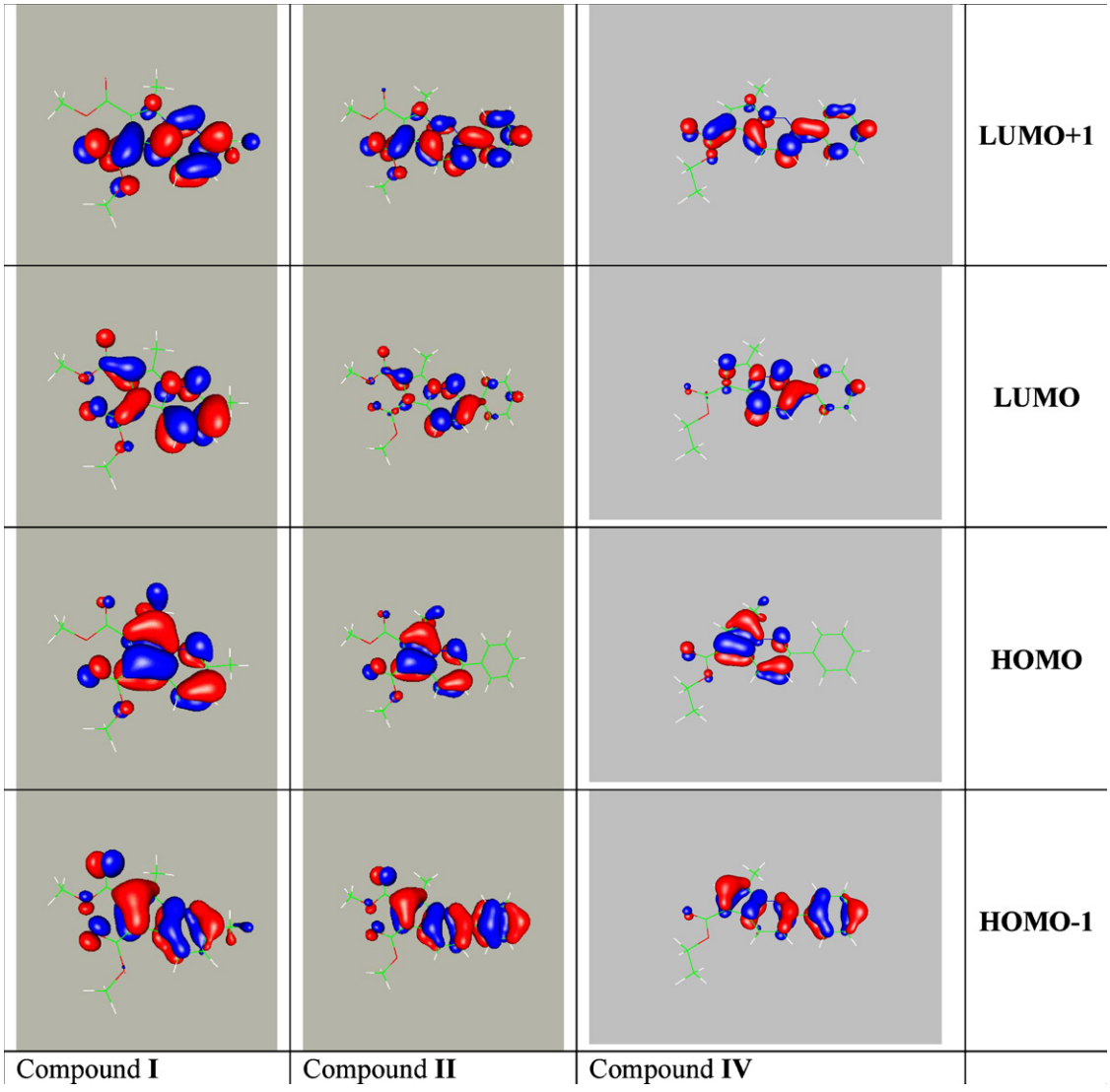

Fig. 2. Isoamplitude surfaces of the MOs of **I**, **II** and **IV**.

to PBE0. These underbinding of the HOMO orbitals is generally traced back to an incorrect asymptotic decay of the xc potential [41,42]. Unexpectedly, the increase of the basis set size from SVP to DZP is slightly increasing the energies of the MOs (see Table 2) by a similar amount for both occupied and unoccupied MOs. However, a further increase of the basis set by employing the triple zeta valence polarized basis is decreasing the energies of the MOs slightly below the values obtained with the SVP basis set.

The calculated absorption spectra of the studied compounds whose spectra appear to be significantly influenced by the substituents at the pyrrolic and pyridazinic rings are presented in Fig. 3 together with the experimental absorption spectra recorded in cyclohexane. The electronic transitions are presented both as line spectra as well as with Gaussian broadening to simulate the experimental spectra and the vibrational broadening that is not included in our present calculations. In addition, the B3LYP and PBE0 electronic transition wavelengths assigned as being mainly responsible for the absorption peaks of **I**, **II**, **III** and **IV** are given also numerically in Table 3 together with their oscillator strengths. The influence of the cyclohexane solvent on the absorption spectra of **I**–**IV** has been tested with both B3LYP/SVP and PBE0/TZVP and is exemplified in Fig. 4.

The comparison of the results obtained with the B3LYP and PBE0 functionals and same basis set reveals that basically the same MOs are involved in the electronic transitions and that a small shift towards shorter wavelengths is observed for PBE0. Increasing the basis set is slightly shifting the absorption towards higher wavelengths. Small variations due to functional and basis set are seen in the MOs contributions of higher energy transitions. This leads to some variations in the assignment of the electronic transitions responsible for the absorption peaks (see gray highlighting in Table 3). However, it is difficult to draw a clear and definitive conclusion on which computational setup is best recommended, especially insofar as the xc functional is concerned.

Employing the COSMO continuum solvatation model for simulating the cyclohexane absorption spectra is inducing only small differences in the absorption wavelengths (<5 nm). Similar results can be expected for other non-polar solvents due to their generally small solute–solvent interactions. The shifts as compared to the vacuum calculations are towards higher wavelengths for B3LYP/SVP and towards lower wavelengths for PBE0/TZVP (see Fig. 4). Additionally, not surprisingly some variations in oscillator strengths and MO contributions of the higher energy transitions are observed for some of the compound.

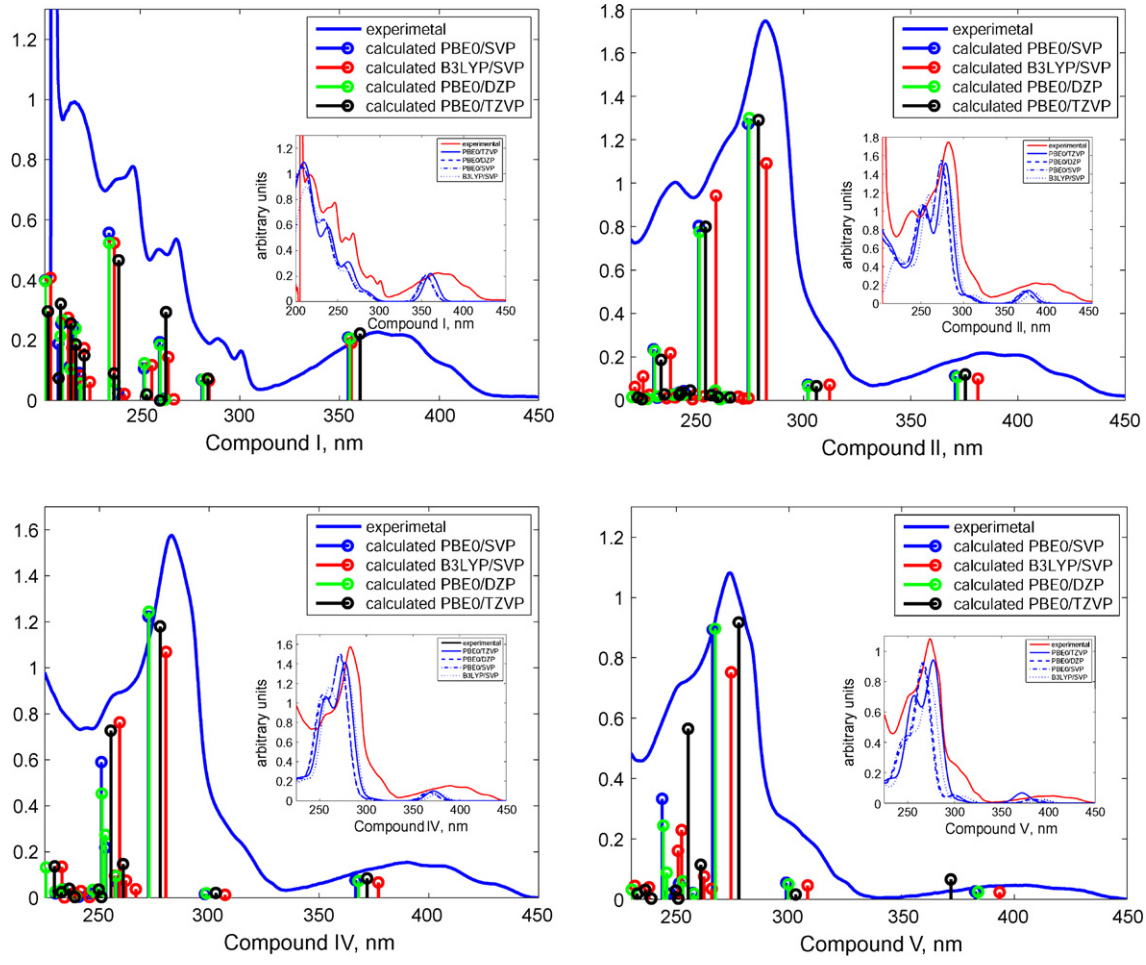

Fig. 3. Calculated absorption spectra of compounds **I**, **II IV** and **V** presented both as line spectra and with Gaussian broadening in the inset.

Table 3
Main calculated electronic transitions corresponding to the experimental absorption peaks of compounds **I**, **II**, **IV** and **V**. The transition wavelengths, oscillator strengths and MOs contributions are given and the differences due to the xc functional and basis set are highlighted with gray

Comp	B3LYP/SVP			PBE0/SVP			PBE0/DZP			PBE0/TZVP			Exp.
	nm	MO	osc. strenght	nm	MO	osc. strenght	nm	MO	osc. strenght	Nm	MO	osc. strenght	nm
I	356	H→L	0.11	354	H→L	0.11	355	H→L	0.11	360	H→L	0.12	380.4
													370.0
													300.6
	285	H-1→L H→L+1	0.04	281	H-1→L H→L+1	0.04	281	H-1→L H→L+1	0.04	284	H-1→L H→L+1	0.04	289.2
	264	H-3→L H→L+1	0.08	260	H-3→L H→L+1	0.10	260	H-3→L H→L+1	0.10	263	H→L+1 H→L+2 H-1→L H-3→L	0.16	268.2
	256	H-3→L H→L+2 H→L+1	0.07	252	H-3→L H→L+2 H→L+1	0.06	252	H-3→L H→L+2 H→L+1	0.06	–	–	–	
	237	H→L+2 H→L+1 H-1→L	0.29	234	H→L+2 H→L+1 H-1→L	0.31	234	H→L+2 H→L+1 H-1→L	0.29	239	H→L+2 H→L+1 H-1→L	0.25	246.4
	Several electronic transitions involving lower lying HOMO orbitals												217.2
	205	H-3→L+2 H-1→L+2	0.22	202	H-3→L+2 H-1→L+2	0.22	202	H-3→L+2 H-1→L+2	0.22	212	H-2→L+1 H-5→L	0.17	
										202	H-3→L+2 H-1→L+2	0.16	
II	381	H→L	0.06	371	H→L	0.06	372	H→L	0.06	376	H→L	0.07	397.6
													384.8
	312	H-1→L H→L+1	0.04	302	H-1→L H→L+1	0.04	302	H-1→L H→L+1	0.04	306	H-1→L H→L+1	0.04	282.4
	283	H→L+1	0.61	274	H→L+1 H-1→L	0.70	275	H→L+1 H-1→L	0.72	278	H→L+1 H-1→L	0.71	
	259	H-1→L+1	0.52	251	H-1→L+1	0.45	251	H-1→L+1	0.43	254	H-1→L+1	0.44	
	238	H→L+3 H-5→L	0.12	230	H→L+3 H-5→L	0.13	231	H→L+3 H-5→L	0.13	233	H→L+3 H-5→L H-3→L 8% contribution H→L+4 8% contribution	0.10	240.4
IV	377	H→L	0.04	367	H→L	0.04	368	H→L	0.04	372	H→L	0.05	390
	280	H→L+1 H-1→L	0.59	272	H→L+1 H-1→L	0.68	273	H→L+1 H-1→L	0.69	278	H→L+1 H-1→L	0.65	283
	259	H-1→L+1 H→L+2	0.42	258	H-2→L H-1→L+1	0.04	252	H-3→L H-1→L+1 H-3→L+1 (11%) H-6→L (8%)	0.15	261	H-2→L H-1→L+1	0.08	244.6
				253	H-3→L H-1→L+1 H-3→L+1 (11%) H-6→L (10%)	0.12	251	H-1→L+1 H-3→L H→L+2 (9%) H-2→L (8%)	0.25	255	H-1→L+1 H-2→L	0.40	
V	393	H→L	0.02	383	H→L	0.02	384	H→L	0.02	389	H→L	0.02	405.4
	274	H→L+1 H-1→L	0.53	266	H→L+1 H-1→L	0.64	267	H→L+1 H-1→L	0.64	272	H→L+1 H-1→L	0.62	274.0
	252	H-1→L+1 H-4→L H-2→L	0.16	244	H-1→L+1 H-2→L	0.23	244	H-1→L+1 H-2→L H-4→L	0.17	248	H-1→L+1 H-2→L	0.2	-
	250	H-4→L H-1→L+1	0.11										

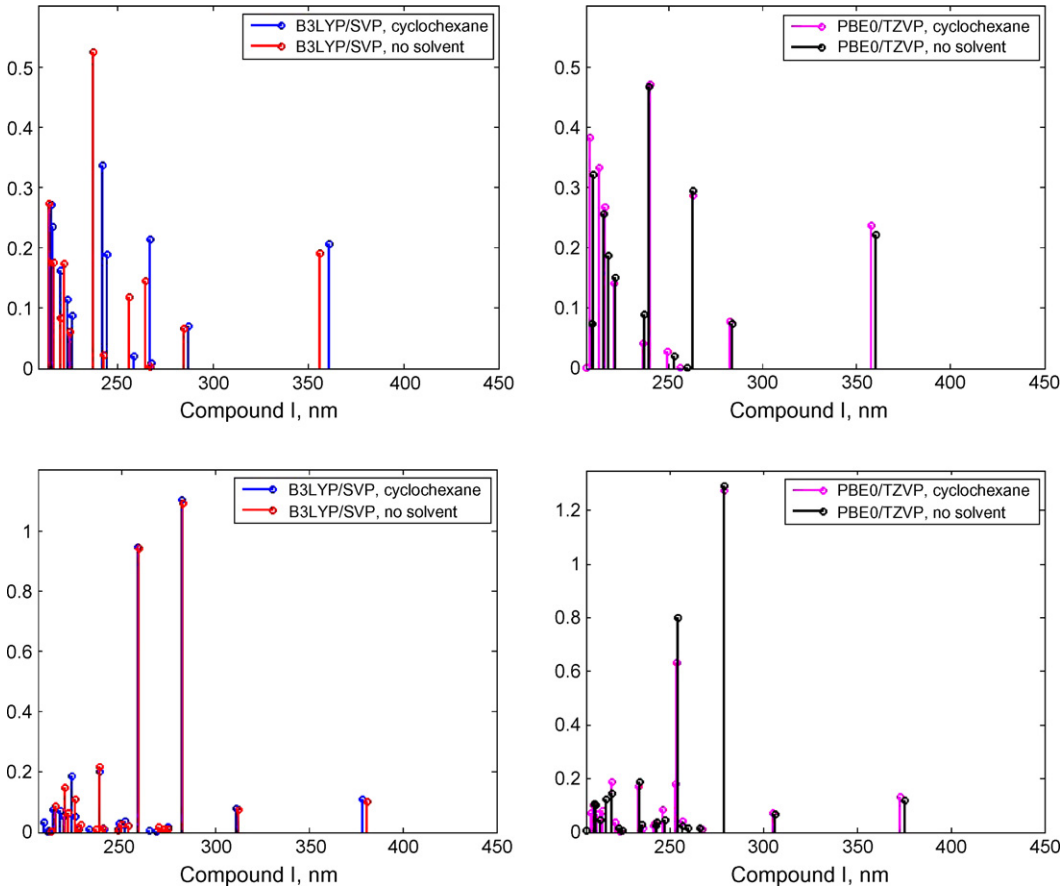

Fig. 4. Electronic excitations calculated for **I** and **II** by employing COSMO continuum solvatation model.

In order to understand the origin of the differences in absorption spectra induced by the substitution of methyl or phenyl to the pyridazinic ring we will closely examine the individual electronic excitations which give rise to the absorptions of **I** and **II**. The highest wavelength absorption peaks of **II** and **I** are red-shifted by ca. 17 nm. The electronic excitation responsible for the absorption involves in both cases a transition from HOMO to LUMO. As detailed above, the energy of HOMO remains basically unchanged when replacing the methyl substituent with phenyl. At the same time, the LUMO energy is lowered significantly. This combined effect is decreasing the HOMO–LUMO gap of **II** as compared to that of **I**, resulting in the observed shift towards higher wavelengths.

The high intensity absorption peak around 280 nm observed in the absorption spectrum of **II** is also present in the absorption spectrum of **I** but with a much lower intensity. The analysis of the data presented in Table 3 reveals that the absorption of **II** around 280 nm is the result of three electronic excitations of which two having high oscillator strengths. The third one is identical in MOs contributions and oscillator strengths to the one leading to the 280 nm absorption of compound **I**. Both compound **I** and **II** exhibit an absorption peak, around 240 nm. However, different MOs are involved in the electronic transitions, thus different oscillator strengths are calculated and observed for the 240 nm absorption. In addition, the spectrum of **I** exhibits also an absorption peak around 217 nm, which is the result of electronic transitions involving low-lying HOMOs and higher LUMOs.

In conclusion, the substitution of methyl by phenyl preserves several of the low-energy (long wavelength) electronic transitions, and the MOs contributions. Higher energy transitions are more strongly influenced by the change in the substituents, evidencing both changes in MO contributions as well as changes in the wavelengths and oscillator strengths. This is due to the fact that the frontier MOs are mainly localized on the pyridazinic ring, while the higher lying MOs are localized on the substituents.

Analysis of Fig. 3 and Table 3 reveals the differences in the absorption spectrum of **II** as compared to **V**. These are mostly due to the addition of two ester groups to the pyrrolic ring of **V** which induces hypsochromic shifts and increased oscillator strengths in both experimental and calculated spectra. Analysis of Table 2 is evidencing the fact that the maximum wavelength absorption, which originates for both **II** and **V** from electronic transitions involving just HOMO and LUMO, is shifted due to the slight increase in the HOMO–LUMO gap induced by the electron withdrawing ester groups. Both HOMO and LUMO are stabilized by the ester groups, however, HOMO slightly more than the LUMO which leads to the increase of the gap. The gradually decrease in absorption wavelengths due to increased number of ester groups is also reported by Mitsumori et al. [15], who is comparing the absorption and fluorescence spectra

of pyrolopyridazine derivatives with three, two and one ester groups at the pyrrole ring. While this seams generally true, it is not in line with the observations drawn when comparing **II** and **IV**. In this case, although the addition of a second ester group to the pyrrolic ring of **IV** is increasing the oscillator strength it is also inducing slight bathochromic (not hypsochromic) shifts. Analysis of Table 2 reveals that as expected, the electron withdrawing ester groups are stabilizing both HOMO and LUMO. However, the HOMO–LUMO gap is slightly decreased due to the larger stabilization of the LUMO as compared to the HOMO.

The peak around 240 nm, which has high intensity in the absorption spectrum of **II** appears only as a shoulder in the absorption of **IV** and is almost invisible in that of **V**. However, all compounds **II**, **IV** and **V** absorb around 240 nm as can be seen from the TD-DFT results presented in Table 3. The increase in oscillator strengths due to the addition of the ester groups can arise either from differences in MOs involved in the transitions or from the larger overlap of the MOs of the ester containing compounds. As shown by the isosurfaces presented in Fig. 2, there can be significant amplitude of the MOs on the ester groups leading to a larger overlap and accordingly larger oscillator strength.

Basically the same considerations as outlined above for compounds **I** and **II** can be drawn also from the comparative analysis of compounds **II**, **IV** and **V**. In the low-energy region basically the same electronic transitions can be identified in the absorption spectra of the compounds. The differences one can observe when comparing the absorption spectra are mainly due to the differences in oscillator strengths of the individual electronic transitions. The origin of the differences in oscillator strengths is revealed when examining the involved orbitals and their spatial distributions, which are influenced by the substituents attached to the pyrrolic rings.

3.5. Fluorescence spectra

All five compounds are intense fluorescent, with high quantum yield values (Table 4), thus being interesting for applications as molecular probes. Fig. 5 presents the absorption, emission and excitation spectra of **IV** in cyclohexane and *n*-hexane. All studied compounds have emission spectra consisting of one

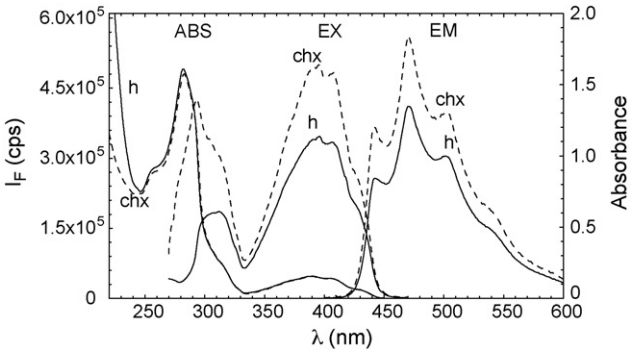

Fig. 5. Absorption, emission and excitation spectra of compound **IV** in cyclohexane (chx) and *n*-hexane (h), $c = 5 \times 10^{-5}$ M.

structured band indicating a planar structure of the molecules, which is in good agreement with the DFT calculated structures. The position of the band is significantly influenced by the replacement of methyl with phenyl in the pyridazinic ring, or by substituting the pyrrolic ring with esters. In the first case a bathochromic shift of $\Delta_{max} = 22$ nm (compare **I** with **II**) and in the second case a hypsochromic shift of $\Delta_{max} = 24$ nm (compare **V** with **II**) can be observed (Table 4). In cyclohexane the fluorescence intensity is higher than in *n*-hexane. For example in the case of compound **IV** the quantum yield is 0.64 in cyclohexane, and 0.43 in *n*-hexane, although the absorption spectra are identical in both solvents (Fig. 5). The results may be explained by the difference in the geometry of the two solvents. Cyclohexane, having fewer degrees of freedom than *n*-hexane, forms a more stable solvatation sphere around the molecules, thus shielding it and stabilizing the excited state. The positions of the excitation spectra bands (Fig. 5) are practically the same as the positions of the absorption bands, however, the long wavelength absorption band is more intense for the fluorescence excitation.

The fluorescence lifetime values, τ, measured at 474 nm for **II**, **III**, **IV** and **V**, and at 460 nm for **I** are presented in Table 4. The fluorescence decay curve of compound **IV** in hexane is shown in Fig. 6. In *n*-hexane the values are higher than in solid state (see Table 4) and the decay curves were fitted with a single-exponential in the solution case, and with a two-exponential function in the solid state case. The two-exponential fit is an indi-

Table 4
Fluorescence parameters: emission maximum wavelength, λ_{mem}, fluorescence quantum yield, Φ, and lifetime, τ, of compounds **I**–**V** in *n*-hexane and solid state; $\lambda_{ex} = 365$ nm. I_f is fluorescence intensity measured in solid state on quartz plate and on powders (values in square brackets)

Compound	λ_{mem} (nm)	Φ	τ (ns)	λ_{mem} (nm) solid	I_f (cps) solid	τ (ns) solid
I	449	0.348	14.14	449 [434]	10897 [50]	0.90 ($a_1 = 33$) 9.85 ($a_2 = 63$)
II	471	0.685	20.96	462 [465]	17299 [65]	4.71 ($a_1 = 23$) 14.28 ($a_2 = 77$)
III	471	0.543	21.07	462 [465]	15974 [73]	3.82 ($a_1 = 24$) 13.94 ($a_2 = 76$)
IV	471	0.434	17.35	462 [465]	19350 [100]	2.18 ($a_1 = 23$) 15.84 ($a_2 = 77$)
V	495	0.122	11.43	517 [509]	596 [5]	–

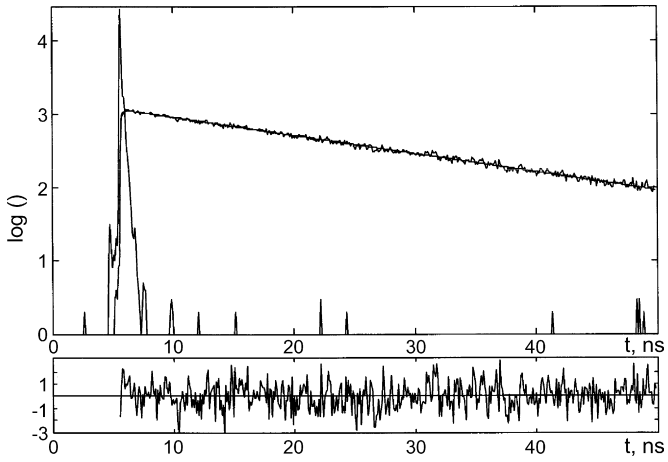

Fig. 6. The fluorescence decay curves of **IV** in *n*-hexane $\lambda_{em} = 500$ nm, laser pulse and random distribution of weighted residuals; on the ordinate are the number of counts.

cation of molecular interactions in solid phase and probably the formation of two geometrical conformers. The pre-exponential values a_1 and a_2, presented in Table 4, are evidencing the percentages of the two conformers. In all the cases $a_2 > a_1$, thereby the fraction of molecules related to the slow component of the fluorescence decay is higher that that of the fast component. Approximately the same values for the pre-exponent a_1 are obtained for the compounds **II**, **III** and **IV**, however, in the case of compound **I** the value of a_1 is higher. We suppose that the methyl and phenyl substituents at the pyridazinic ring are responsible for the observed difference, i.e. the phenyl substituents can induce a deviation from co-planarity to a small part of the molecules during the evaporation of cyclohexane. The packing of the molecules in solid state is influenced by the mentioned substituents. Additionally, the molecular stacking and arrangement in solid state are also influenced by the strong dipole–dipole interactions between the ester moieties.

For the solid state case one can observe the same influence of the substituents as in solution (Fig. 7 and Table 4): the position of the band is influenced when methyl is replaced by phenyl in pyridazinic ring (bathochromic shift of 13 nm), or when substituting esters to the pyrrolic ring (hypsochromic shift of 55 nm, if compare **V** with **II**). The difference $\Delta\lambda$ in the emission maximum wavelength λ_{mem} obtained by comparing the solid state and the solution emission is negative (−9 nm) for the compounds **II**, **III** and **IV**, zero for **I**, and positive for **V** (22 nm). The hypsochromic shift is due a week π–π interaction in the case of compounds **II**, **III** and **IV** favored by the effect of the substituents (especially carboethoxy or carbomethoxy) and the phenyl at the pyridazinic ring. In the case of **I**, which has methyl substituted at the pyridazinic ring no shift is observed ($\Delta\lambda = 0$). In the case of **V**, $\Delta\lambda$ is positive because there are no ester substituents and the π–π intermolecular interaction is stronger. The fluorescence intensity of **V** is lower both in solution and solid state. Strong π–π interactions effectively quench the fluorescence in solid state as is also concluded in [43]. It should be mentioned that the values of the fluorescence intensity in solid state given in Table 4 are only approximate. The uniformity of the layer could not be easily controlled and it is therefore not possible to have absolute values, although the measurements have been made by frontal face illumination. The measurements for powders of compounds have also been done by frontal face illumination. The results are presented in brackets (in Table 4). One can observe that the tendency of the fluorescence intensity variation is the same as in the case of the thin layer of crystalline compounds.

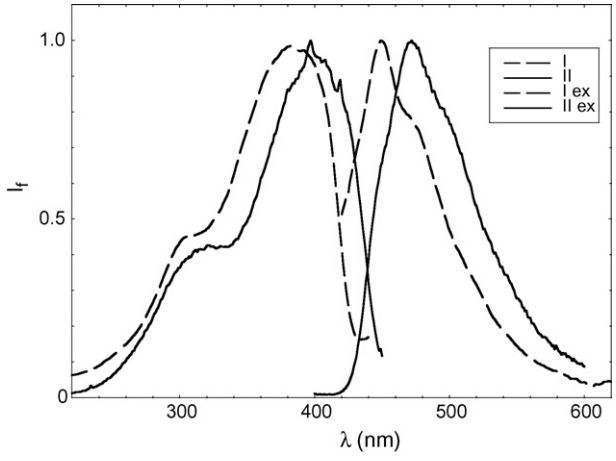

Fig. 7. Emission ($\lambda_{ex} = 365$ nm) and excitation spectra of compounds **I** ($\lambda_{em} = 449$ nm) and **II** ($\lambda_{em} = 465$ nm) in solid state.

The co-planarity of pyrrolopyridazine with the phenyl ring (compounds **II**–**V**) was evidenced in solid state by X-ray analysis in the case of very close analogues [16] of **V**. The π-stacking interaction between molecules with interplanar distance of 3.40 Å are strong enough for possible applications requiring high electronic mobility.

4. Conclusions

The investigation of the absorption spectra and steady-state fluorescence of the pyrrolo[1,2-b]pyridazine derivatives **I**–**V** in cyclohexane and *n*-hexane solutions, as well as in solid state, has evidenced important modifications induced by the substituents. Bathochromic shifts have been observed for **II**, **III** and **IV** when compared with **I**, and are attributed to the extent of the conjugation of the π-electrons. The hypsochromic shift, observed if one compares **II** with **V**, evidences the important role of the substitution of esters to the pyrrolic ring. From density functional theory and time dependent DFT calculations of the absorption spectra of **I**–**V** one can conclude that basically the same electronic transitions can be identified in the low-energy region of the absorption spectra of the compounds. The experimentally observed differences are mainly due to the differences in oscillator strengths of the individual electronic transitions. The origin of the differences in oscillator strengths is revealed when examining the involved MOs and their spatial distributions, which are influenced by the different substituents. COSMO calculations show in the case of cyclohexane only small differences as compared to the vacuum calculated spectra.

All five compounds are intense fluorescent, with high quantum yield values (in *n*-hexane): 0.35 (**I**), 0.69 (**II**), 0. 54 (**III**), 0.44 (**IV**) and 0.12 (**V**), values which reflect the increase of

the conjugation of double bonds in the cases of **II** and **III**, compared with **I** and the fluorescence enhancement effect of the ester substituents. The fluorescence decay data could be fitted to a mono-exponential function for solutions and to double-exponential function for compounds in solid state. The double-exponential decay could be due to the existence of two distinct geometrical conformations in the solid state of the compounds. In *n*-hexane the τ values are higher than in solid state. The steric requirements of the substituents are the main cause of the spectral changes of the absorption and fluorescence maxima in the solid state compared with the solutions. The difference in emission maximum wavelength between solid state and solution, $\Delta\lambda$, is negative (−9 nm) for the compounds **II**, **III** and **IV**, zero for **I** and positive for **V** (22 nm).

In the view of these considerations and the results presented above several more general conclusions can be drawn regarding the influence of the nature and position of the substituents on the properties and absorption spectra of pyrrolopyridazine derivatives. Optical absorption and fluorescence spectra are, not surprisingly, independent on the alkyl substituents at the pyrrolic ring, unless their steric requirements are not influencing the solid state spectra. The expansion of the π-system due to substitutions at the pyridazinic ring is inducing bathochromic shifts and is increasing fluorescence quantum yields and lifetimes. The addition of ester groups and presumably other electron withdrawing groups to the pyrrolic ring have in general an opposite effect on the absorption and fluorescence wavelengths evidenced by hypsochromic shifts. At the same time these substituents can significantly increase absorption intensities, which can resolve additional peaks in the spectrum. Thus, one can conclude that the present study provides a first basis for the prediction of the spectroscopic properties of other similar pyrrolopyridazine derivatives.

Acknowledgements

This contribution has been financed by Romanian Academy and most of the data have been obtained thanks to a co-operation program between Romanian Academy and the Academy of Finland.

References

[1] C.W. Tang, S.A. VanSlyke, Appl. Phys. Lett. 51 (1987) 913.
[2] P.E. Burrows, S.R. Forrest, Appl. Phys. Lett. 64 (1994) 2285.
[3] G. Horowitz, Adv. Mater. (Weinheim Ger.) 10 (2000) 365.
[4] J.H. Burroughes, D.D.C. Bradley, A.R. Brown, R.N. Marks, K. Mackay, R.H. Friend, P.L. Burns, A.B. Holmes, Nature 347 (1990) (1990) 539.
[5] A. Dodabalapur, L. Torsi, H.E. Katz, Science 268 (1995) 270.
[6] F. Garnier, G. Horowitz, D. Fichou, A. Yassar, Supramol. Sci. 4 (1997) (1997) 155.
[7] D.Y. Zang, S.R. Forrest, IEEE Photonics Technol. Lett. 4 (1992) 365.
[8] D.Y. Zang, Y.Q. Shi, F.F. So, S.R. Forrest, W.H. Steier, Appl. Phys. Lett. 58 (1991) 562–564.
[9] R.B. Taylor, P.E. Burrows, S.R. Forrest, IEEE Photonics Technol. Lett. 9 (1997) 365.
[10] M. Vasilescu, R. Bandula, F. Dumitrascu, H. Lemmetyinen, J. Fluorescence 16 (2006) 631–639.
[11] M. Vasilescu, R. Bandula, F. Dumitrascu, H. Lemmetyinen, Spectrophotometric characteristics of new pyridylindolizine derivatives in solid state, in: 5th International Conference of the Chemical Societies of the South-East European Countries (ICOSEC 5), Ohrid, Macedonia, September 10–13, 2006.
[12] M. Vasilescu, F. Dumitrascu, H. Lemmetyinen, N. Tkachenko, J. Fluorescence 14 (2004) 443.
[13] M. Vasilescu, R. Bandula, F. Dumitrascu, C. Draghici, H. Lemmetyinen, Rev. Roum. Chim. 49 (2004) 905–910.
[14] Y. Cheng, B. Ma, F. Wudl, J. Mater. Chem. 9 (1999) 2183–2188.
[15] T. Mitsumori, M. Bendikov, J. Sedo, F. Wudl, Chem. Mater. 15 (2003) 3759–3768.
[16] M. Caira, F. Dumitrascu, C. Draghici, D. Dumitrescu, M. Cristea, Molecules 10 (2005) 360–366.
[17] K.M.K. Swamy, M.S. Park, S.J. Han, S.K. Kim, J.H. Kim, C. Lee, H. Bang, Y. Kim, S.-J. Kim, J. Yoon, Tetrahedron 61 (2005) 10227–10234.
[18] E.A. Meade, L.L. Wotrin, J.C. Drach, L.B. Townsend, J. Med. Chem. 36 (1993) 3834–3842.
[19] W. Malinka, Pharmazie 56 (2001) 384–389.
[20] O.B. Østby, L.L. Gunderson, F. Rise, O. Antonsen, K. Fosnes, V. Larsen, A. Bast, I. Custers, G.R.M.M. Haenen, Arch. Pharm. Pharm. Med. Chem. 334 (2001) 21–24.
[21] J.M. Ruxer, C. Lachoux, J.B. Ousset, J.L. Torregrosa, G.J. Mattioda, J. Heterocycl. Chem. 31 (1994) 409–417.
[22] M. Ungureanu, L. Mangalagiu, G. Grosu, M. Petrovanu, Ann. Pharm. Fr. 55 (1997) 69–72.
[23] A.I. Nassir, L.L. Gundersen, F. Rise, O. Antonsen, T. Kristensen, B. Langhelle, A. Bast, I. Custers, G.R.M.M. Haenen, H. Wikstrom, Bioorg. Med. Chem. Lett. 8 (1998) 1829–1832.
[24] O.B. Østby, B. Dalhus, L.L. Gundersen, F. Rise, A. Bast, G.R.M.M. Haenen, Eur. J. Org. Chem. 22 (2000) 3763–3770.
[25] M. Pal, V.R. Batchu, S. Khanna, K.R. Yeleswarapu, Tetrahedron 38 (2002) 9933–9940.
[26] F. Dumitrascu, C. Mitan, D. Dumitrescu, C. Draghici, M.T. Caproiu, M. Vasilescu, 10-th Blue Danube Symposium on Heterocyclic Chemistry, Vienna, Austria, PO-126, September 3–6, 2003.
[27] W.H. Melhuish, J. Phys. Chem. 65 (1961) 229;
W.H. Melhuish, J. Opt. Soc. Am. 54 (1964) 183–188.
[28] H. Caldararu, A. Caragheorgheopol, M. Vasilescu, I. Dragutan, H. Lemmetyinen, J. Phys. Chem. B 98 (1994) 5320.
[29] S.H. Vosko, L. Wilk, M. Nusair, Can. J. Phys. 58 (1980) 1200.
[30] P.A.M. Dirac, Proc. Royal Soc. 123 (1929) 714.
[31] J.C. Slater, Phys. Rev. 81 (1951) 385.
[32] C. Lee, W. Yang, R.G. Parr, Phys. Rev. B 37 (1988) 785.
[33] A.D. Becke, J. Chem. Phys. 98 (1993) 5648.
[34] J.P. Perdew, K. Burke, M. Ernzerhof, Phys. Rev. Lett. 77 (1996) 3865.
[35] J.P. Perdew, M. Ernzerhof, K. Burke, J. Chem. Phys. 105 (1996) 9982.
[36] M. Cossi, V. Barone, J. Chem. Phys 115 (2001) 4708.
[37] A. Schäfer, H. Horn, R. Ahlrichs, J. Chem. Phys. 97 (1992) 2571.
[38] T.H. Dunning Jr., Chem. Phys. 90 (1989) 1007.
[39] N. Godbout, D.R. Salahub, J. Andzelm, E. Wimmer, Can. J. Chem. 70 (1992) 560.
[40] R. Ahlrichs, M. Bär, M. Häser, C. Kälmel, Chem. Phys. Lett. 162 (1989) 165.
[41] G.E. Adamo, V. Scuseria, Barone, J. Chem. Phys. 111 (1999) 2889.
[42] R.E. Stratmann, G.E. Scuseria, M.J. Frisch, J. Chem. Phys. 109 (1998) 8218.
[43] K. Shirai, M. Matsuoka, K. Fukunishi, Dyes Pigments 42 (1999) 95.